Supporting Information

Kinetic Theory for Formation of Diamond Nanothreads with Desired Configurations: Strain-Temperature Controlled Phase Diagram

Junfeng Gao[1], Gang Zhang[1], Boris I. Yakobson[2], Yong-Wei Zhang[1†]*

[1] Institute of High Performance Computing, A*STAR, Singapore 138632

[2] Department of Materials Science and Nano Engineering, Rice University, Houston, Texas 77005, United States

---

* Email: zhangg@ihpc.a-star.edu.sg

† Email: zhangyw@ihpc.a-star.edu.sg

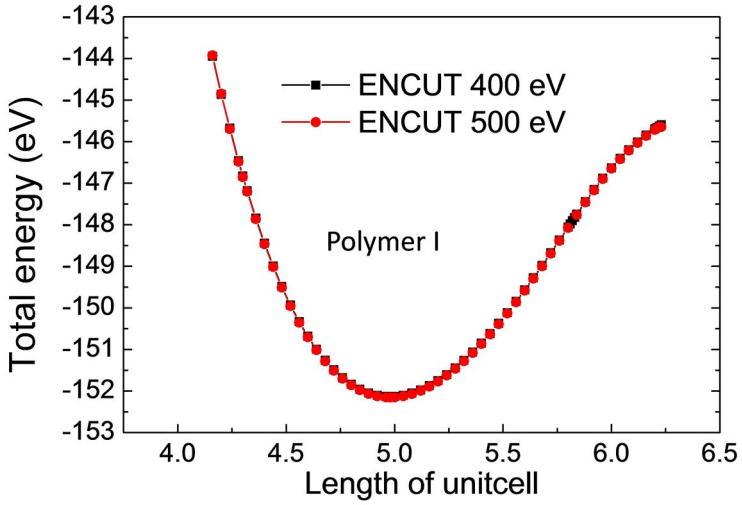

Figure S1 | Energy cutoff test for DNTs. We have calculated energy-length curves for polymer-I using energy cutoff of both 400 eV and 500 eV. Figure S1 shows the results obtained at 400 eV and 500 eV agree with each other very well. Only near fracture point, there is a slight difference between these two curves. In our work, we choose 500 eV for the structure and stress-strain curve calculation.

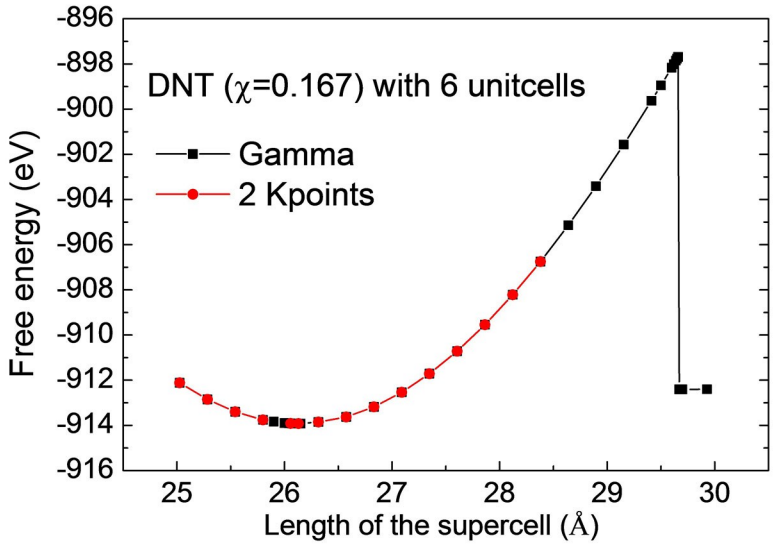

Figure S2 | k-mesh test for DNTs. For the model including more than 6 unit cells (over 25.8 Å), we use only Gamma point for sampling in reciprocal space. For the DNT(χ=0.167) with 6 unit cells, we also relax its structure and calculate the total energy using 2 ***k***-point sampling along the periodic length direction. These two results match each other perfectly, indicating that Gamma point sampling is enough for the study of DNTs with supercell length over 25.8 Å. This can be explained by the factor that DNTs are wide bandgap systems.

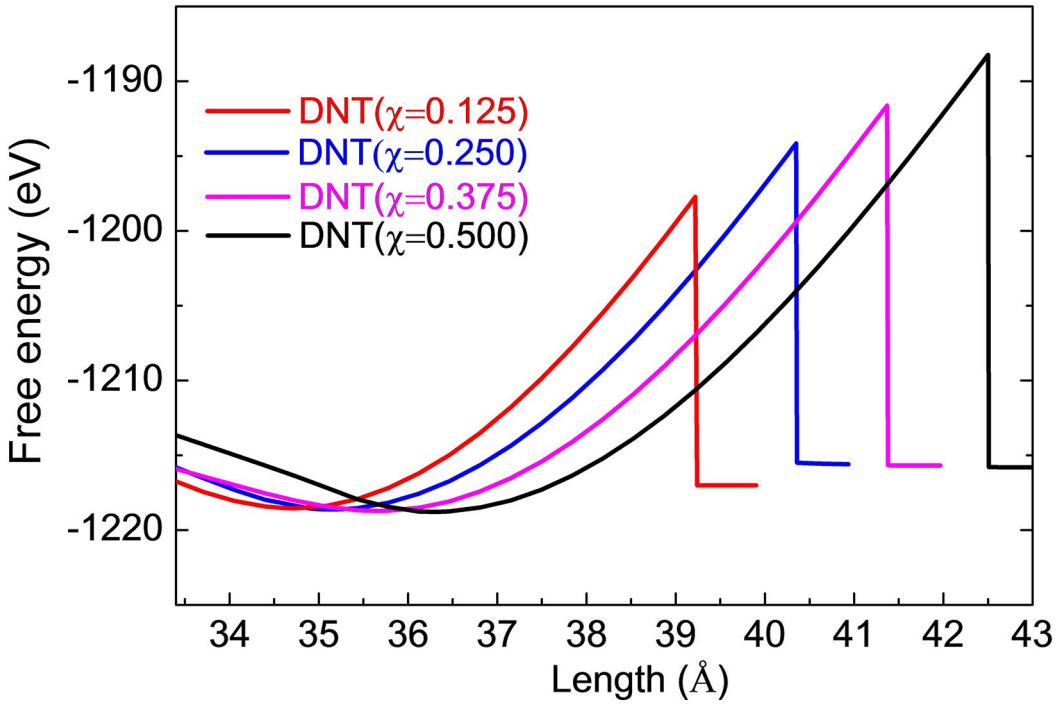

Figure S3 | Total energy change of DNT(χ=0.125, 0.250, 0.375, 0.500) with length. From χ=0.125 to χ= 0.500, the equilibrium energy of DNT gradually decreases.

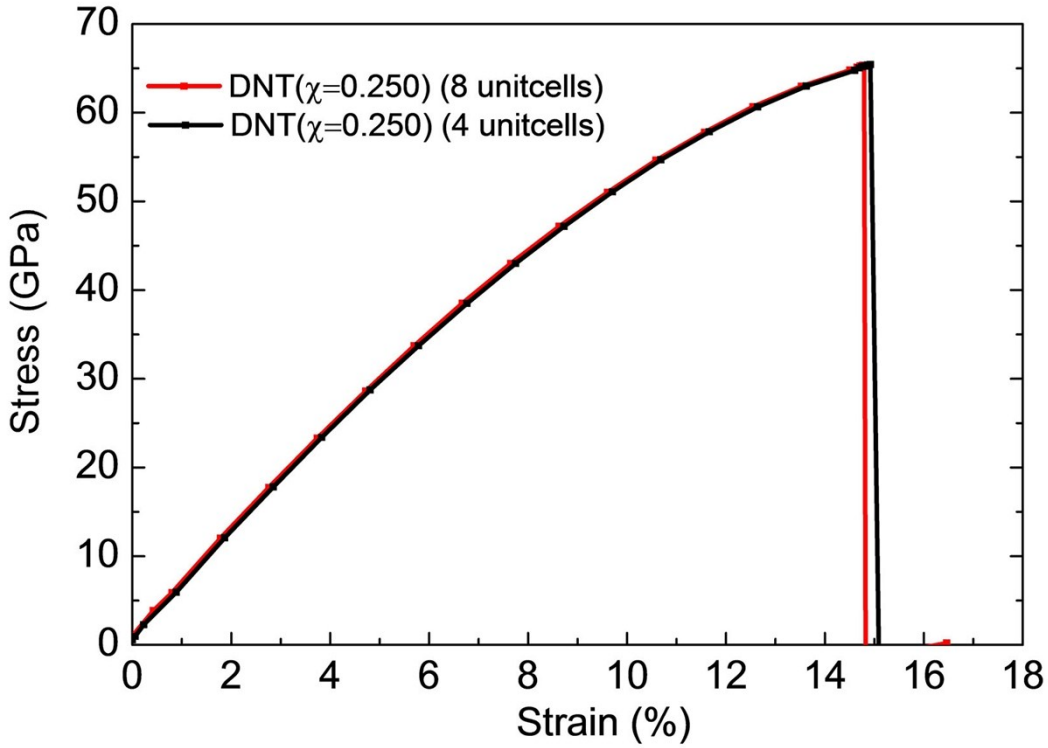

Figure S4 | Comparison of the stress-strain curves of DNT(χ=0.250) between 4- and 8- unit cells. We have calculated the stress-strain of DNTs with the same χ but different total lengths. It is seen that these two cases almost have the same yield stress at the same yield strain. Therefore, for the models with periodic boundary condition used here, the length does not influence the accuracy of the results.

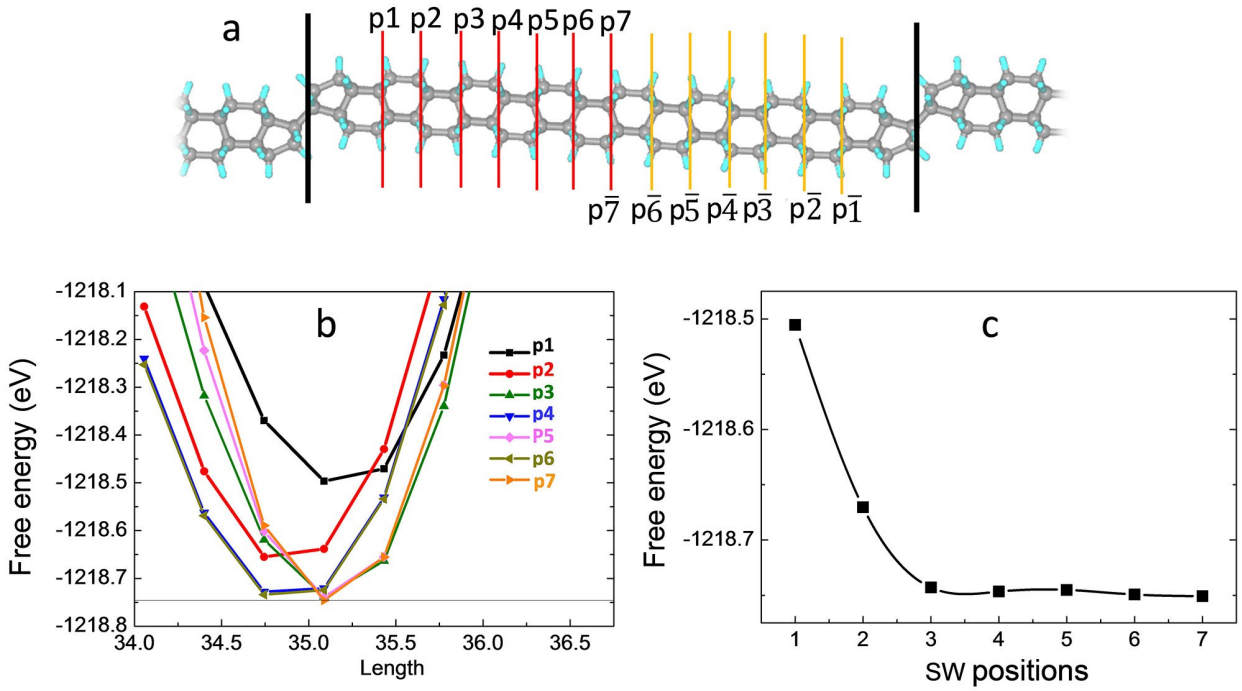

Figure S5 | The free energy of DNT varying with the relative position of two SW transformations. We have relaxed and calculated the different SW distances using 8-unitcell modes. Their energy-length curves are shown in Fig. S5b. After the generation of the first SW transformation, the second SW transformation is positioned at different positions, p1-p7. Here p1 is the nearest position to the first SW transformation. Clearly, p1 and p2 positions possess the highest and second highest energies, respectively. With increasing the distance, p3-p7 have the similar equilibrium energy, and p7 is slightly lower than others. Besides, the equilibrium length of p3, p5, and p7 is longer than that of p4 and p6. Therefore, p3, p5, and p7 are more stable in tension. From these result, we can conclude that the direct connection of two SWs is not energetically favored until χ=50%.

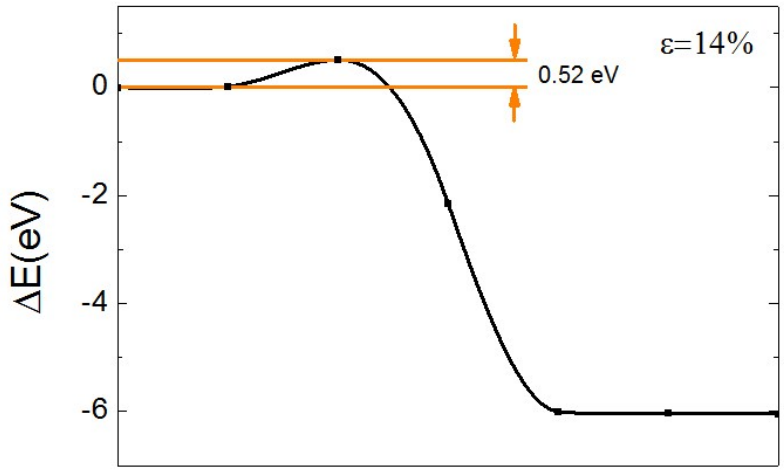

Figure S6 | SW transformation barriers. The SW transition path and energy barrier under 14% tensile strain.

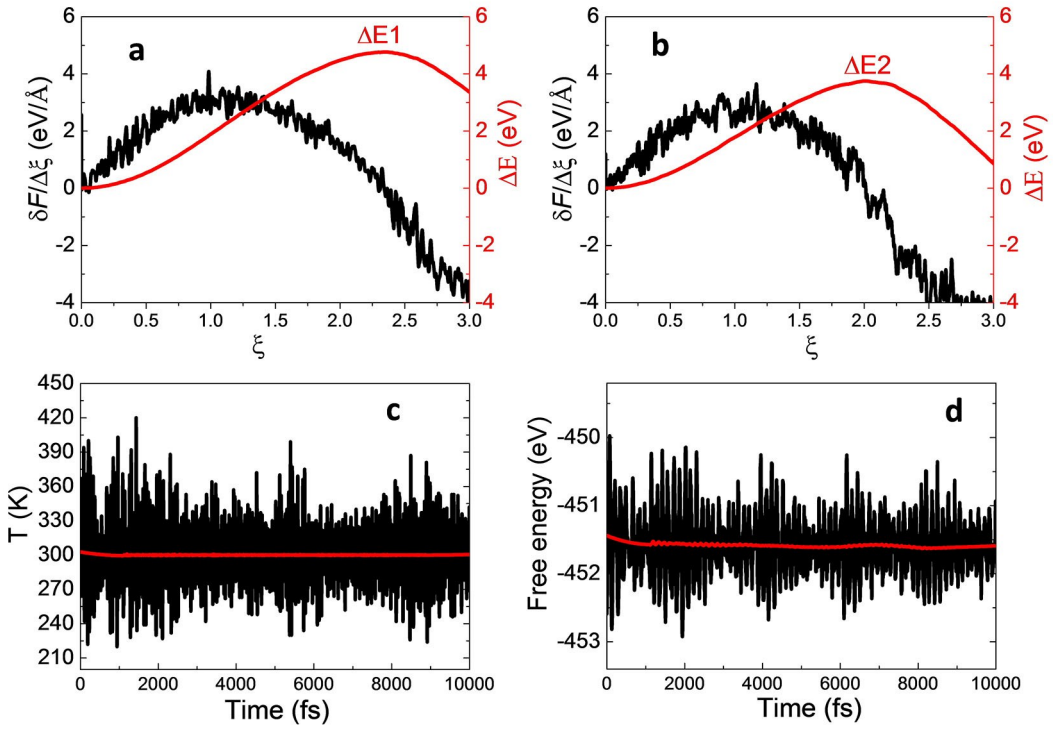

Figure S7 | SW transformation using CAIMD simulations. The energy gradient (black line) and total energy change (red line) for the first C-C bond rotation (a) and second C-C bond rotation (b). The temperature in CAIMD is 300 K. The corresponding trajectories for (a) and (b) are provided in Supporting video-1 and video-2, respectively. After the rotation, the DNT with SW transformation is simulated using normal AIMD with NVT ensemble at 300 K. The system reaches equilibrium state quickly and the structure of DNT is stable in another 10 ps simulation as shown in Figure S7c, d. The trajectory for the 10 ps normal AIMD simulation is provided in Supporting video-3 and video-4.

S11 | Total energy changing of DNTs during a sequence of SW occurs as in Figure 5d&5e

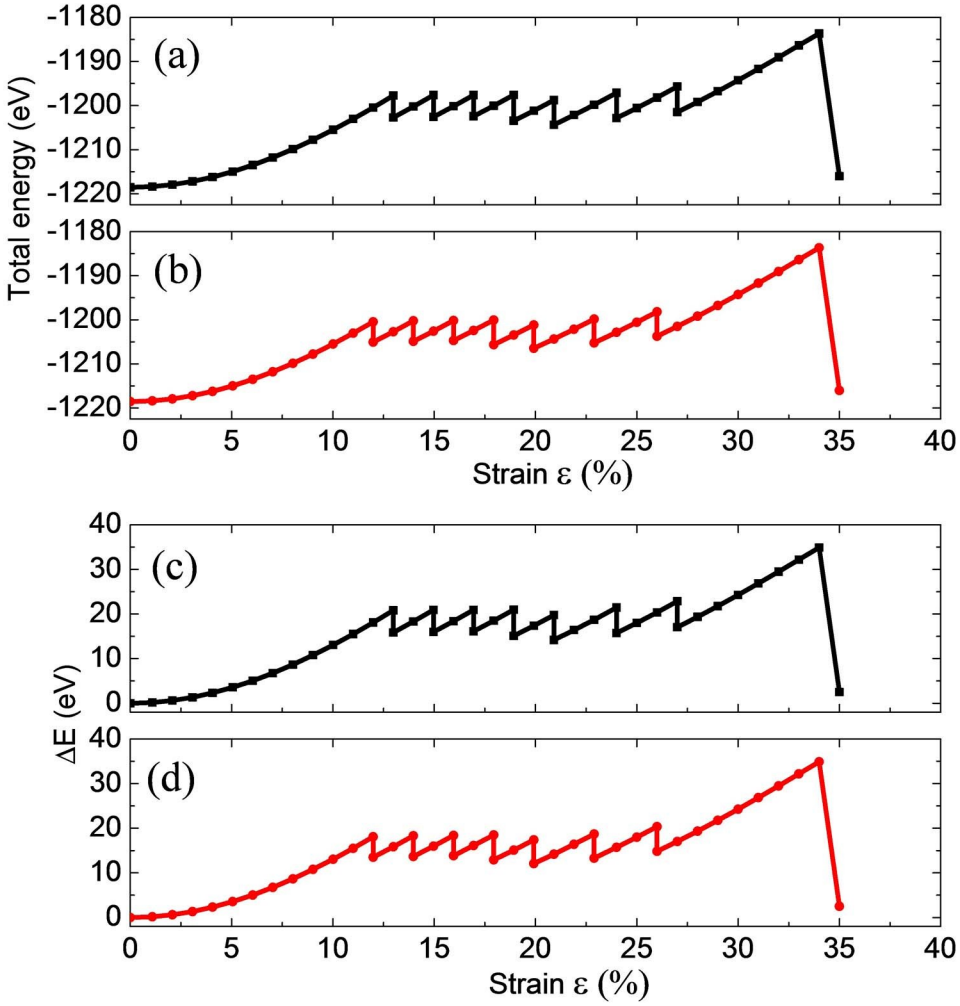

Figure S11. The change in total energy as a function of strain in 8-unitcell $DNT_{i/8}$, (i=1…8) at the strain of (a) 12.5% and (b) 13%. The corresponding energy differences during these transitions at the strain of (c) 12.5% and (d) 13%.

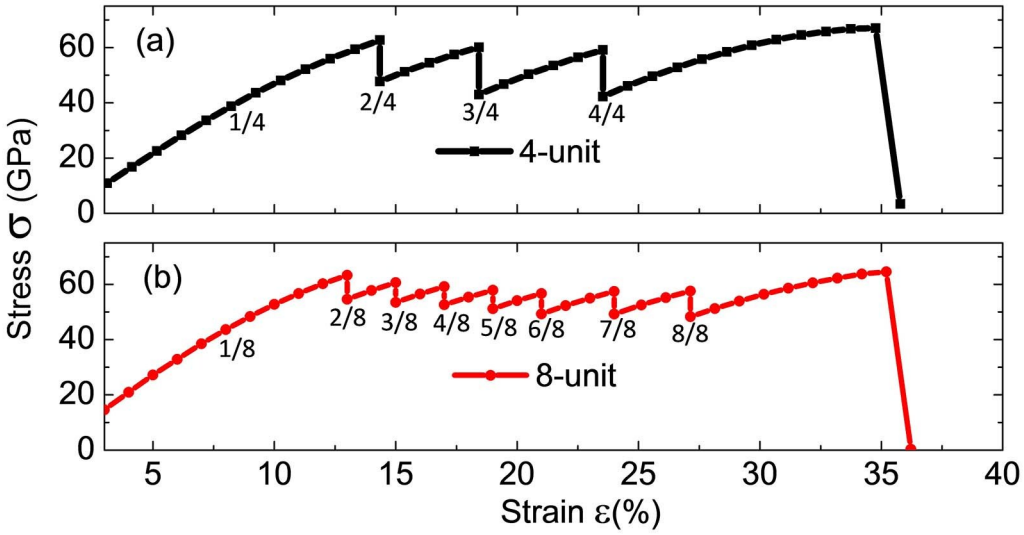

Figure S12 | Comparison of SW transition in 4-unit (a) and 8-unit (b) supercells.

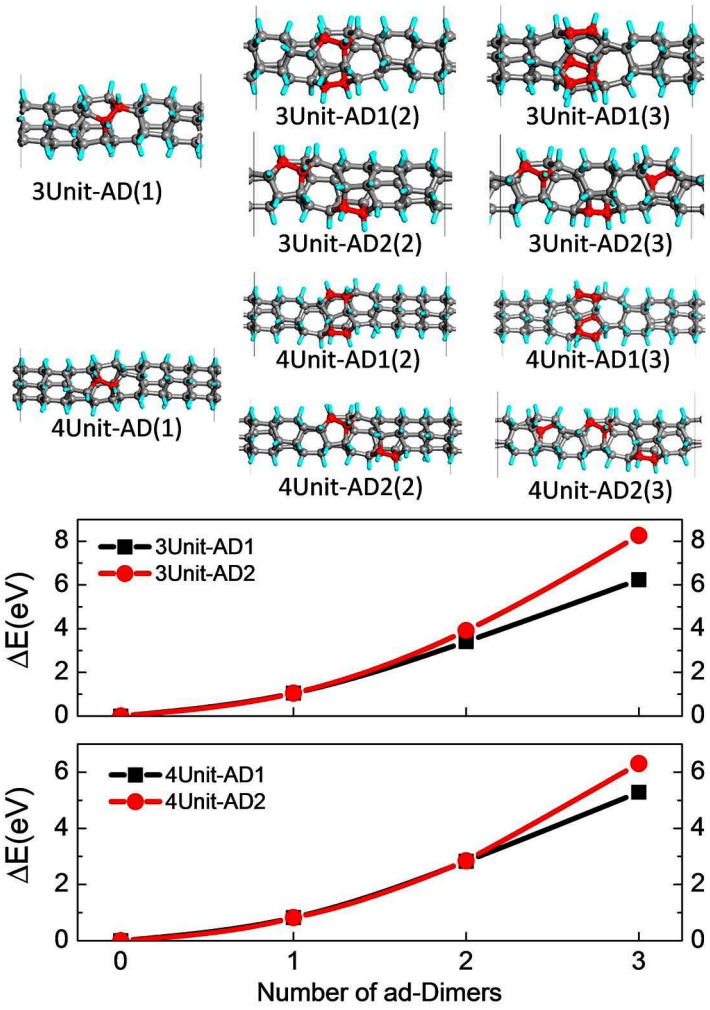

Figure S13 | The structures and formation energies of AD-dimer in 3unit- and 4unit-DNTs. AD1 and AD2 represent radial and axial distribution of AD. It is interesting the AD-dimer with radial diffusion is more popular than that with axial distribution. However, different from SW lower the energy of DNT below χ=0.500, AD-dimer increases the formation energy of DNT significantly. One AD-dimer increases 0.82 eV (1.05 eV) of the formation energy for 4 unit (3 unit) supercell H-tube(3,0). Three AD-dimers forming defective circles in 4 unit (3 unit) H-tube(3,0) increases the total formation energy to 6.31 (8.27) eV, thus lowering the stability of DNTs greatly.

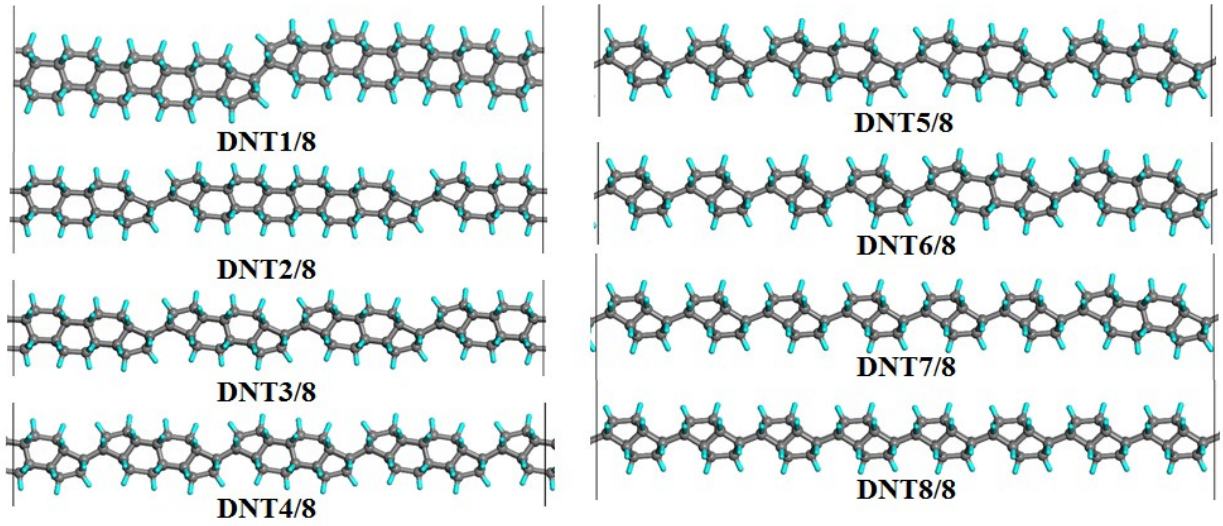

Figure S14 | Structures of $DNT_{i/8}$ (i=1-8) we explored.